JOC The Journal of Organic Chemistry

Editors' Choice

pubs.acs.org/joc

Article

Molecular Dynamics of the Norbornyl Cation in Solution and Its Generation in Winstein−Trifan Solvolysis: The Timing of Sigma Bridging

Woojin Lee, Tyler R. Benton, Arkajyoti Sengupta, and K. N. Houk*

Cite This: J. Org. Chem. 2024, 89, 1140−1146

Read Online

ACCESS | Metrics & More | Article Recommendations | Supporting Information

ABSTRACT: Molecular dynamics simulations were performed on the solvolyses of *exo*- and *endo*-norbornyl brosylate and for the "nonclassical" σ-bridged norbornyl cation in an acetic acid solution. This computational modeling of the original Winstein−Trifan experiment confirms that *exo*-solvolysis is accompanied by σ-bridging in the transition state, while *endo*-solvolysis is not; σ-bridging eventually occurs in a dynamically stepwise fashion. Simulations of the norbornyl cation in solution show typical vibrations due to zero-point and thermal vibrations but no tendency to sample localized "classical cation" geometries.

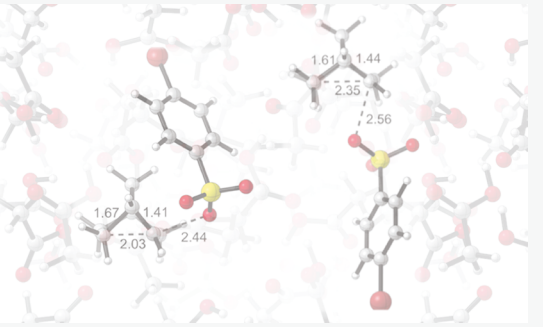

INTRODUCTION

Bridged cations are now a widely accepted type of carbocation intermediates.[1] It was not always so!

In 1949, Winstein and Trifan reported the acetolysis of *exo*- and *endo*-2-norbornyl brosylates.[2,3] They observed that the *exo*-isomer solvolyzed 350 times faster than the *endo*-isomer. Only the racemic *exo*-2-norbornyl acetate product was formed (Figure 1A). The authors proposed a three-center, two-electron structure of 2-norbornyl cation (Figure 1B). Its formation occurred during solvolysis only by backside C−C "anchimeric assistance" in the *exo*-solvolysis. A plane of symmetry in the delocalized carbonium ion allows the attack of acetate at C_1 or C_2 with equal probability, giving racemic *exo*-norbornyl acetate.

Moreover, anchimeric assistance by the interaction of the C_1-C_6 σ-bond with the σ* anti-bonding orbital between C_2 and the leaving group's oxygen was proposed to explain the faster solvolysis of 2-*exo*-norbornyl brosylate. Roberts, who coined the term *nonclassical* cations, proposed that the bridged 2-norbornyl cation might be viewed as a 3-fold symmetric nortricyclonium ion.[4] In the early 1960s, Brown began to publish objections to the Winstein interpretations and invoked equilibrating "classical" cations to rationalize racemization and steric effects to explain the greater rate of *exo*-solvolysis (Figure 1C).[5,6]

Meanwhile, Olah and co-workers employed nuclear magnetic resonance (NMR) methods to observe 2-norbornyl cation in magic acid solutions (SbF_5/SbF_5-SO_2/SbF_5-SO_2ClF-SO_2F_2).[7] They discovered that hydride shifts are frozen out at −158 °C. The structure of the 2-norbornyl cation was proposed to be a symmetrically bridged structure **1** or a structure in rapid equilibrium (≤3 kcal/mol) between localized cations **2** and **3**. The results obtained at −268 °C by Yannoni et al. indicated a single-minimum bridged structure or rapid equilibration between the classical cations through an

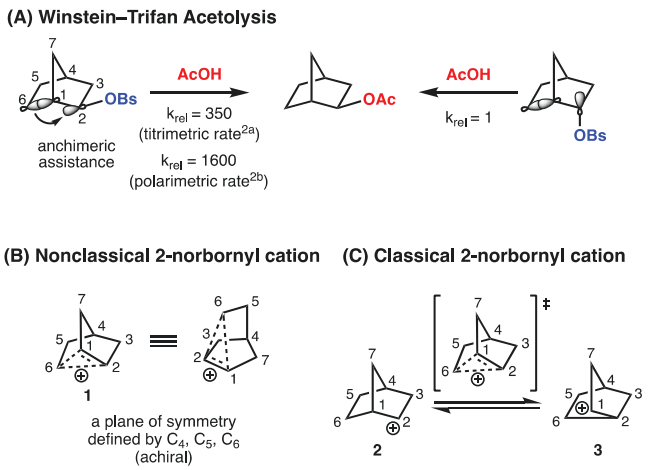

Figure 1. (A) Winstein−Trifan acetolysis. (B) Nonclassical 2-norbornyl cation. (C) Classical 2-norbornyl cation.

Received: October 12, 2023
Revised: December 5, 2023
Accepted: December 12, 2023
Published: December 30, 2023

https://doi.org/10.1021/acs.joc.3c02325
J. Org. Chem. 2024, 89, 1140−1146

extremely low energy barrier (<0.2 kcal/mol).[8] Saunders et al. used isotopic perturbation methods to demonstrate that the 2-norbornyl cation is a single symmetrical structure.[9] Schleyer, Schreiner, Schaefer, Jorgensen, et al. compared the stability of the symmetrically bridged (C_s) structure **1** and classical structures **2** and **3** with ab initio quantum mechanical methods. They predicted the significant stabilization of the symmetric 2-norbornyl cation and showed that the classical structure is not a minimum.[10,11] Monte−Carlo simulation studies in force-field water predicted the lower energy of the nonclassical ion, even with highly polar water solvation. Meyer, Krossing, et al. decisively confirmed the symmetrically bridged structure of the 2-norbornyl cation, albeit in the solid state, via X-ray crystallography.[12] List and co-workers demonstrated enantiocontrol over the nonclassical 2-norbornyl cation with imidodiphosphorimidate catalysts, induced by a chiral anion.[13]

The structure of the norbornyl cation was definitively established in the solid state and in the gas phase. Only (to some) the nagging question of whether the classical cation might be more stabilized in solution remained, in spite of Jorgensen's convincing solution simulations. In earlier work, Schreiner et al. modeled the Winstein experiment, employing water as a leaving group instead of brosylate, and conducted the study in the gas phase.[19] Their findings found the presence of bridging in the *exo*-transition state, but not in the *endo*-transition state. The question of the timing of σ-bridging in acetic acid, the Winstein−Trifan solvent, has not been explored computationally. We have now studied the cation in solution and the Winstein−Trifan solvolysis reaction in acetic acid with the brosylate leaving group (Figure 1A) using modern quantum mechanics and molecular dynamics techniques.

COMPUTATIONAL METHODS

All density functional theory (DFT) computations were performed with Gaussian 16.[14] Geometry optimizations were performed at the M06−2X/6−311+G(d,p) level of theory.[15] Frequency calculations were carried out at the same level of theory used for geometry optimization to characterize stationary points as minima or saddle points on the potential energy surface (PES) and to obtain Gibbs free energies at 298 K. The Solvation Model based on Density (SMD) was employed to account for AcOH solvation.[16] The 3D molecular structures are visualized here by CYLView[17] and PyMol.

MD simulations of solvolysis were performed at the M06−2X/6−31G(d)/SMD=AcOH level of theory. The Progdyn/Gaussian interface developed by Singleton was employed to perform trajectory simulations.[18] Quasiclassical trajectories were initialized near the saddle point region of the PES with a normal-mode sampling method (Figure 2). This method involves adding zero-point and thermal energy for each real normal mode in the TS and obtaining a Boltzmann distribution by randomly sampling a set of geometries and velocities. The transition state ensemble was propagated for 500 fs. The time step for integration was 1 fs. The norbornyl cation was studied in implicit SMD solvation and also in explicit acetic acid solvent with M06−2X/6−31G(d).

RESULTS AND DISCUSSION

We evaluated the energies of forming a norbornyl cation from *exo*- and *endo*-norbornyl brosylates with M06−2X/6−311+G(d,p)/SMD=AcOH (Figure 3A). *Exo*-norbornyl brosylate **SM$_{exo}$** is more stable than *endo*-norbornyl brosylate **SM$_{endo}$**. The ionization of *exo*-norbornyl brosylate **TS1a** occurs with a free energy of activation of 24.0 kcal/mol, while **TS1b** for *endo*-norbornyl brosylate ionization has an activation free energy of 26.0 kcal/mol. The ionization of the *exo*-norbornyl brosylate is

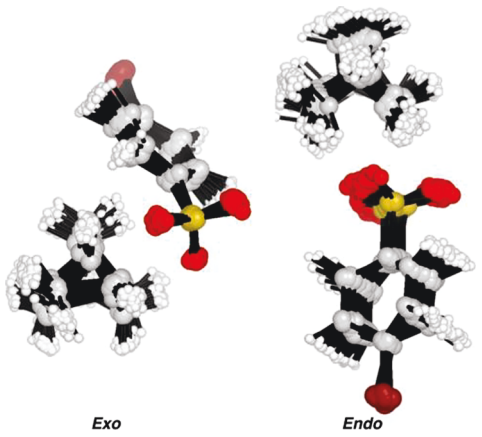

Figure 2. Transition state ensembles of *exo*- and *endo*-solvolysis of norbornyl-2-brosylate.

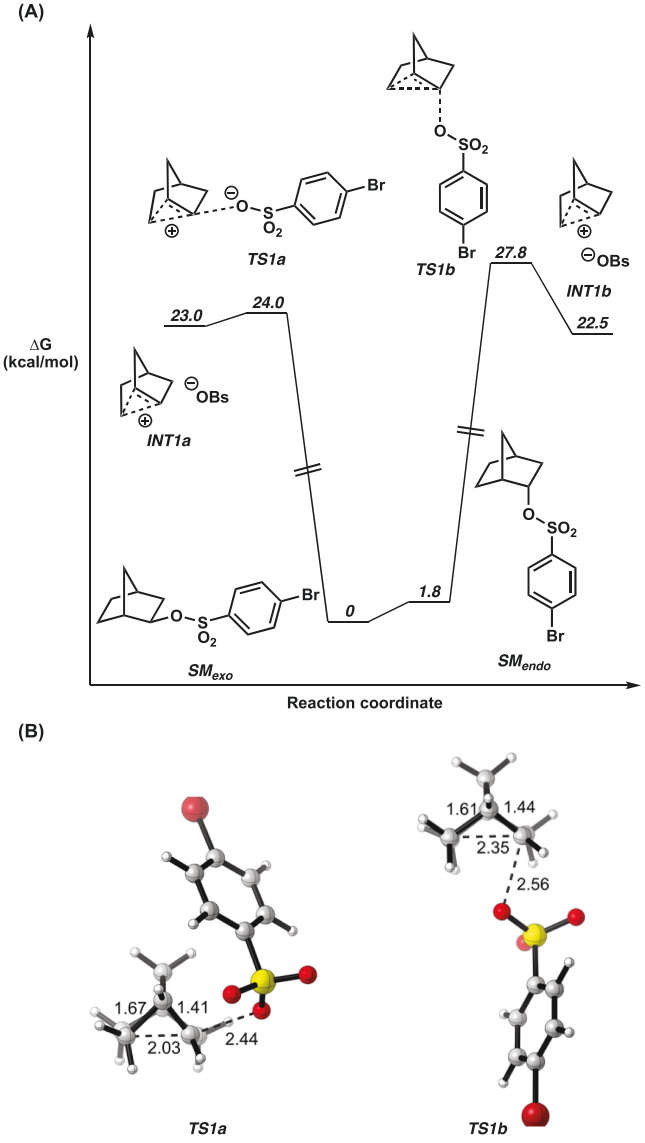

Figure 3. (A) Energy profile of *exo*- and *endo*-norbornyl brosylate solvolysis. (B) Transition states of *exo*- and *endo*-solvolysis.

favored by 2 kcal/mol. This computational result resembles the original titrimetric ratio (k_{exo}/k_{endo} = 350, $\Delta\Delta G^{\ddagger} \sim$ 3.5 kcal/

https://doi.org/10.1021/acs.joc.3c02325
J. Org. Chem. 2024, 89, 1140−1146

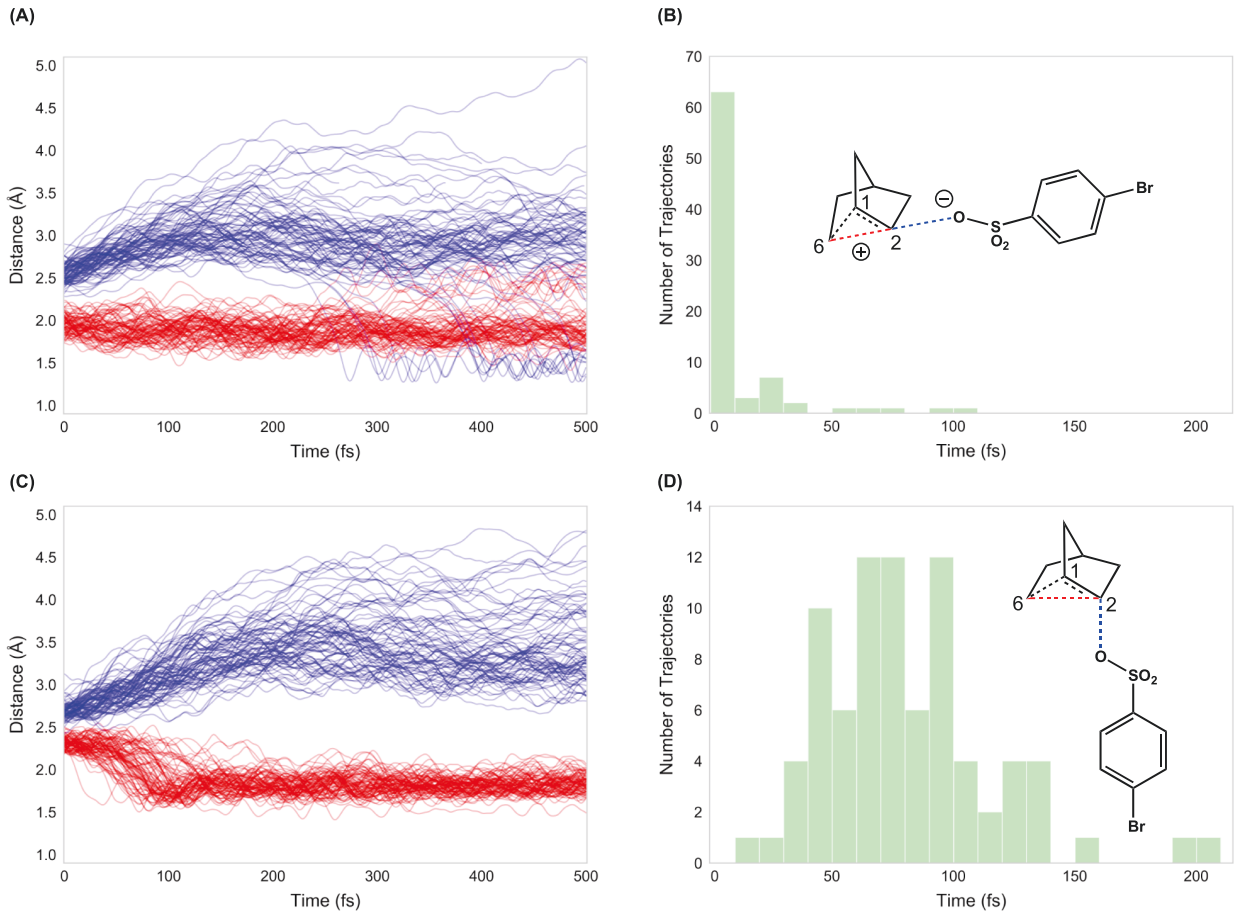

Figure 4. (A) C_6-C_2 (red) and C_2-O (blue) distances during *exo*-solvolysis trajectories. (B) Histogram of time-to-bridging during *exo*-solvolysis trajectories. (C) C_6-C_2 and C_2-O distances during *endo*-solvolysis trajectories. (D) Histogram of time-to-bridging during *endo*-solvolysis trajectories.

mol) obtained by Winstein and Trifan.[2] The transition state structures of **TS1a** and **TS1b** are shown in Figure 3B. Anchimeric assistance helps the ionization of norbornyl cation from *exo*-norbornyl brosylate.[2] Note bond lengths of 2.03 and 2.35 Å of C_6-C_2 in **TS1a** and **TS1b,** respectively. The C_6-C_2 bond distance in *exo*-solvolysis **TS1a** shows substantial bridging in the transition state. The σ orbital of C_6-C_2 donates electron density to σ^* orbital of C_2-O through antiperiplanar interactions. The rate of *exo*-solvolysis in the formation of the 2-norbornyl carbocation is accelerated by anchimeric assistance. In contrast, bridging does not occur in the *endo*-norbornyl solvolysis **TS1b**, although there is some hyperconjugation as indicated by C_6-C_1 and C_1-C_2 bond lengths of 1.61 and 1.44 Å, respectively.

The steric strain difference between the *exo*- and *endo*-transition states invoked by Brown is very modest. In the case of *exo*-solvolysis **TS1a**, the distance between oxygen in the leaving group and the nearest hydrogen in C_3 is 2.48 Å, while the closest O---H distance is 2.23 Å in *endo*-solvolysis **TS1b**, indicative of van der Waals contacts (see Supporting Information for more details).

In order to study the timing of σ-bridging, we employ Singleton's Progdyn program for quasiclassical molecular dynamics simulations with DFT (M06−2X/6−31G(d)/SMD=AcOH).

We measured the time to form the bridged C_6-C_2 bond from the *exo*- and *endo*-solvolysis transition states. The bridging distance is determined as 2.00 Å, proposed by Schreiner et al.[19] According to Eyring's transition state theory, the pre-exponential factor, kT/h, is defined by the rate of translational motion of atoms. A time of 60 fs is the lifetime of a typical transition state at room temperature. We consider the formation of a bridged bond (≤2.00 Å) to be dynamically concerted if the time is ≤ 60 fs. Conversely, if the time is > 60 fs, it is considered to be a dynamically stepwise process.[20] We ran 80 trajectory simulations with *exo*-transition states. As shown in Figure 4A, most of the trajectories showed the formation of a bridged bond near the beginning of the simulations. Seventy-six trajectories show the dynamically concerted formation of bridged cations (Figure 4B), and only four trajectories show the dynamically stepwise formation of bridged cations. The average timing of the bridged bond formation from the *exo*-solvolysis transition states is 9 fs. The solvolysis of *exo*-norbornyl brosylate occurs through a dynamically concerted process.

For *endo*-solvolysis, 81 trajectory simulations were performed. Figure 4C shows the noticeable change in the C_6-C_2 bond distance at 81 ± 68 fs. As shown in Figure 4D, 58 trajectories show the dynamically stepwise formation of bridged cations, while 23 trajectories are dynamically concerted. The average time to form a bridged C_6-C_2 bond from *endo*-transition states is 81 ± 68 fs, indicating a dynamically stepwise process on average.

https://doi.org/10.1021/acs.joc.3c02325
J. Org. Chem. 2024, 89, 1140−1146

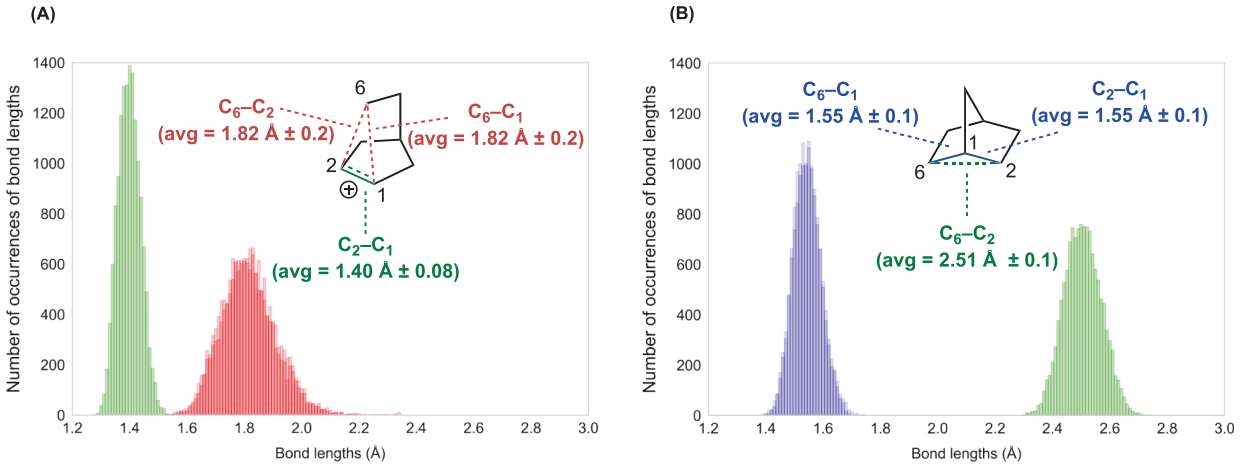

Figure 5. (A) Histograms of C_6-C_2 and C_6-C_1 (red), and C_2-C_1 (green) bond lengths during 2-norbornyl cation 29 500 fs trajectory simulations. (B) Histograms of C_6-C_1 and C_2-C_1 (blue), and C_6-C_2 (green) bond distances during norbornane 26 500 fs trajectory simulations.

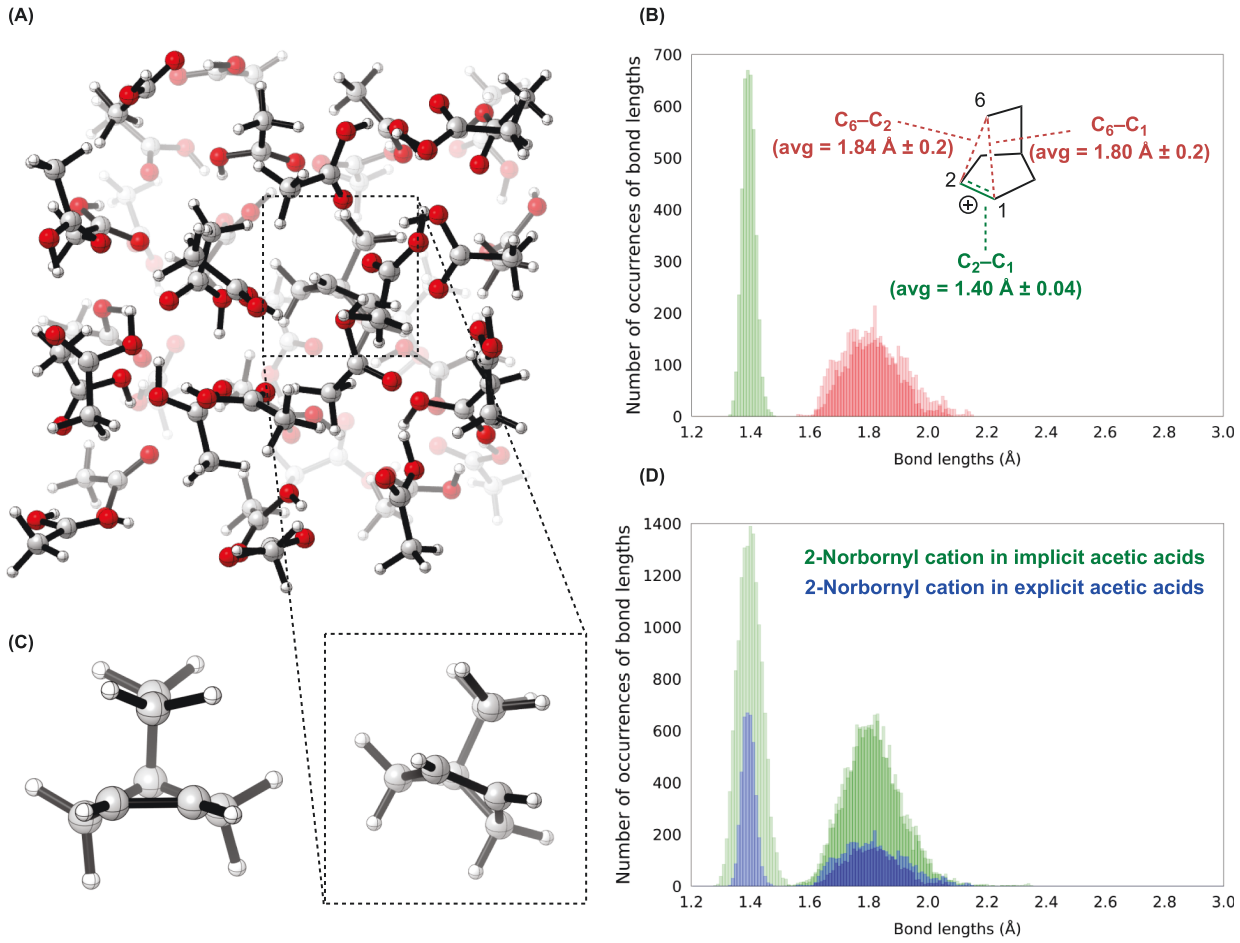

Figure 6. (A) Snapshot from 2-norbornyl cation simulation in explicit acetic acid solution. (B) C_6-C_2 and C_6-C_1 (red) and C_2-C_1 (green) bond lengths during 2-norbornyl cation 4 1000 fs trajectory simulations. (C) Snapshot from 2-norbornyl cation simulation in implicit acetic acid solution. (D) Histogram overlay of 2-norbornyl cation simulations between implicit (green) and explicit (blue) solutions.

While the distinction of the timing of σ-bridging seems very subtle (81 vs 9 fs is 7×10^{-14} s), this is the difference between bridging stabilization of the rate-determining transition state (0–9 fs) and what occurs only after several C–C vibrations after the transition state, which is not, therefore, stabilized by bridging.

Ion-pair recombination is also observed in the simulations of *exo*-solvolysis. Fourteen trajectories showed covalent bond reformation (C_2-O) after the formation of a bridged C_6-C_2 bond. Note that the C_2-O bond distance is decreased to ~ 1.5 Å, as shown in Figure 4A. Recombination occurs because of the low energy gap (ΔG = 1.0 kcal/mol) between **INT1a** and

https://doi.org/10.1021/acs.joc.3c02325
J. Org. Chem. 2024, 89, 1140–1146

TS1a (Figure 3A) and corresponds to internal return in solvolysis.

We also investigated the behavior of the norbornyl cation in acetic acid solvent at ambient temperature (Figure 5A). Previous studies were performed in force-field water, where the lifetime of the cation would be very small.[11] We simulated molecular dynamics of the ground-state norbornyl cation with 29 trajectories (500 fs for each trajectory). The average bond length of C_6-C_1 and C_6-C_2 is 1.82 ± 0.2 Å. Figure 5A shows the histogram of bridging partial single bonds, with a bin size of 0.01 Å from 1.50 to 2.39 Å. Fully 86.3% of these bond distances fall within the range of 1.70−1.99 Å, while the remaining 13.7% are outside this range. Schleyer's computational work showed that the bond distance of C_6-C_1 in the classical 2-norbornyl cation is 1.55 Å.[10] Our simulations find that only 0.06% of C_6-C_1 or C_6-C_2 bonds are equal to or less than 1.55 Å, characteristic of the classical 2-norbornyl cation. Pemberton and Tantillo studied lifetimes of classical secondary carbocations of bornyl, presativyl, and preprezizyl cations using molecular dynamics simulations.[21] We find that classical 2-norbornyl cations are a negligible component of norbornyl cations in solution. The average bond length of C_2-C_1 is 1.40 ± 0.08 Å, typical of 50% double-bond character, as in an aromatic ring.

We also performed molecular dynamics with norbornane to compare its C−C bond behavior with the partial sigma bonds of the 2-norbornyl cation. We simulated 26 trajectories (500 fs for each trajectory). The results are summarized in Figure 5B. The C_2-C_1 bond lengths of 1.55 ± 0.1 Å varied in length about half that for the C_6-C_2 or C_6-C_1 bonds of the norbornyl cation. This is consistent with the weaker bonds in the norbornyl cation. The C_6-C_2 distance, 2.51 ± 0.1 Å, similarly varies less in norbornane.

Finally, the 2-norbornyl cation was investigated in explicit acetic acid solution (Figure 6). Only four trajectory simulations were performed with the M06−2X/6−31G(d) level of theory and 40 acetic acids in a box. The setup was obtained by optimization and frequency calculations on the 2-norbornyl cation in the explicit acetic acid environment employing Packmol[22] and ONIOM(M06−2X/6−31G(d)/PM7). Considering an equilibration phase, the simulations are propagated over 1500 fs, and the initial 500 fs from each simulation was excluded. The average bond lengths of C_6-C_1, C_6-C_2, and C_1-C_2 are 1.80 ± 0.2, 1.84 ± 0.2, and 1.40 ± 0.04 Å, respectively (Figure 6B). The analysis of the bond lengths through molecular dynamics in both implicit and explicit acetic acids features a three-center, two-electron structure of a 2-norbornyl cation (Figure 6C and D). The computed average bond lengths of C_6-C_1, C_6-C_2, and C_2-C_1 in solution state are essentially identical to those in the X-ray structures reported by Meyer, Krossing, et al.[12]

CONCLUSIONS

We revisited the Winstein−Trifan solvolysis with DFT and Progdyn MD simulations. The energy difference between *exo*- and *endo*-solvolysis barriers matches Winstein−Trifan's original kinetics. Formation of the C_6-C_2 bridged bond from the *exo*-solvolysis transition state ensemble occurs at 0−9 fs (dynamically concerted). Formation from *endo*-solvolysis happens at 81 ± 68 fs (dynamically stepwise). The solution structure of the norbornyl cation is the same as that in the X-ray crystal structure and never resembles the putative classical norbornyl cation.

ASSOCIATED CONTENT

Data Availability Statement

The data underlying this study are available in the published article and its Supporting Information.

Supporting Information

The Supporting Information is available free of charge at https://pubs.acs.org/doi/10.1021/acs.joc.3c02325.

Energies and Cartesian coordinates of all optimized structures and transition state structures (PDF)

Endo-solvolysis trajectory in SMD acetic acid (MP4)

Molecular dynamics trajectory of norbornyl cation in implicit SMD acetic acid (MP4)

Molecular dynamics trajectory of norbornyl cation in explicit acetic acid (MP4)

Exo-solvolysis trajectory in SMD acetic acid (MP4)

AUTHOR INFORMATION

Corresponding Author

K. N. Houk − *Department of Chemistry and Biochemistry, University of California, Los Angeles, California 90095-1569, United States;* orcid.org/0000-0002-8387-5261; Email: houk@chem.ucla.edu

Authors

Woojin Lee − *Department of Chemistry and Biochemistry, University of California, Los Angeles, California 90095-1569, United States;* orcid.org/0000-0002-8531-0301

Tyler R. Benton − *Department of Chemistry and Biochemistry, University of California, Los Angeles, California 90095-1569, United States*

Arkajyoti Sengupta − *Department of Chemistry and Biochemistry, University of California, Los Angeles, California 90095-1569, United States;* orcid.org/0000-0002-9917-2472

Complete contact information is available at: https://pubs.acs.org/10.1021/acs.joc.3c02325

Notes

The authors declare no competing financial interest.

ACKNOWLEDGMENTS

We are grateful to the National Science Foundation (CHE-1764328 and CHE-2153972) for financial support of this research. K.N.H. thanks the Winstein family and UCLA for the honor and financial support of the Saul Winstein Chair in Organic Chemistry from 2009 to 2021. The support and friendship from Carolee Winstein and Kip Thorne were major inspirations for this work. We also thank Dr. Cooper Jamieson for the helpful comments and discussions pertaining to Progdyn simulations. All calculations were performed on computational resources provided by the UCLA Institute of Digital Research and Education and the NSF Extreme Science and Engineering Discovery Environment.

REFERENCES

(1) (a) Anslyn, E. V.; Dougherty, D. A. *Modern Physical Organic Chemistry*; University Science Books: Herndon, VA, 2006, pp. 661−666. (b) Vogel, P.; Houk, K. N. *Organic Chemistry: Theory, Reactivity and Mechanisms in Modern Synthesis*; Wiley-VCH: Weinheim, Germany, 2019, pp. 308−312. see especially pp. 6907. (c) Naredla, R. R.; Klumpp, D. A. Contemporary Carbocation Chemistry: Applications in Organic Synthesis. *Chem. Rev.* **2013**, *113*, 6905−

6948. (d) Gutta, P.; Tantillo, D. J. Theoretical Studies on Farnesyl Cation Cyclization: Pathways to Pentalenene. *J. Am. Chem. Soc.* **2006**, *128*, 6172−6179. (e) Hong, Y. J.; Tantillo, D. J. Perturbing the Structure of the 2-Norbornyl Cation through C−H···N and C−H···π Interactions. *J. Org. Chem.* **2007**, *72*, 8877−8881. (f) Tantillo, D. J. The Carbocation Continuum in Terpene Biosynthesis−Where are the Secondary Cations? *Chem. Soc. Rev.* **2010**, *39*, 2847−2854.

(2) (a) Winstein, S.; Trifan, D. S. The Structure of the Bicyclo [2,2,1]2-Heptyl (Norbornyl) Carbonium Ion. *J. Am. Chem. Soc.* **1949**, *71*, 2953. (b) Winstein, S.; Clippinger, E.; Howe, R.; Vogelfanger, E. The Nonclassical Norbornyl Cation[1]. *J. Am. Chem. Soc.* **1965**, *87*, 376−377. (c) Winstein, S.; Trifan, D. S. Neighboring Carbon and Hydrogen. X. Solvolysis of endo-Norbornyl Arylsulfonates[1,2,3]. *J. Am. Chem. Soc.* **1952**, *74*, 1147−1154.

(3) The Winstein-Trifan experiments were performed in what is now known as Haines Hall at UCLA, one of the four original 1929 buildings on campus. The Department of Chemistry and Biochemistry now occupy Young, Molecular Sciences, and Boyer buildings. Haines Hall is now occupied by the Departments of Sociology, Anthropology, the Chicano Studies Center, and the Ralph J. Bunche Center for African American Studies.

(4) (a) Roberts, J. D.; Lee, C. C. The Nature of the Intermediate in the Solvolysis of Norbornyl Derivatives[1,2]. *J. Am. Chem. Soc.* **1951**, *73*, 5009−5010. (b) Roberts, J. D.; Mazur, R. H. The Nature of the Intermediate in Carbonium Ion-Type Interconversion Reactions of Cyclobutyl, Cyclopropylcarbinyl, and Allylcarbinyl Derivatives[1]. *J. Am. Chem. Soc.* **1951**, *73*, 3542−3543.

(5) (a) Brown, H. C. (with comments by Schleyer, P. V. R.) *The Nonclassical Ion Problem; Plenum*: New York, 1977. (b) Brown, H. C.; Morgan, K. J.; Chloupek, F. J. Structural Effects in Solvolytic Reactions. I. The Role of Equilibrating Cations in Carbonium Ion Chemistry. Nature of the Intermediates Involved in the Solvolysis of Symmetrically Substituted β-Phenylethyl Derivatives[1]. *J. Am. Chem. Soc.* **1965**, *87*, 2137−2153. (c) Brown, H. C. The Energy of the Transition States and the Intermediate Cation in the Ionization of 2-Norbornyl Derivatives. Where is the Nonclassical Stabilization Energy? *Acc. Chem. Res.* **1983**, *16*, 432−440. (d) Brown, H. C.; Chloupek, F. J.; Rei, M-H. Rates of Solvolysis of the *p*-Nitrobenzoates of *exo-endo* Tertiary Norborneols. A Critical Examination of the *exo-endo* Rate Ratio as a Basis for the Postulated Nonclassical Structure of the Norbornyl Cation. *J. Am. Chem. Soc.* **1964**, *86*, 1248−1250.

(6) (a) Olah, G. A. My Search for Carbocations and Their Role in Chemistry (Nobel Lecture). *Angew. Chem., Int. Ed.* **1995**, *34*, 1393−1405. (b) Olah, G. A.; Schleyer, P. V. R.; Eds. *Carbonium Ions*; Wiley-Interscience: New York, 1968−1976; Vols. *I*−*IV*; (c) Olah, G. A. *Carbocations and Electrophilic Reactions*; Verlag Chemie: Weinheim, 1974. (d) Olah, G. A.; Prakash, G. K. S.; Sommer, J. *Superacids*; Wiley-Interscience: New York, 1985. (e) Olah, G. A.; Molnár, Á. *Hydrocarbon Chemistry*; Wiley-Interscience: New York, 1995. (f) Olah, G. A.; Prakash, G. K. S.; Williams, R. E.; Field, L. D.; Wade, K. *Hypercarbon Chemistry*; Wiley-Interscience: New York, 1987.

(7) (a) Schleyer, P. V. R.; Watts, W. E.; Fort, R. C.; Comisarow, M. B.; Olah, G. A. Stable Carbonium Ions. X.[1] Direct Nuclear Magnetic Resonance Observation of the 2-Norbornyl Cation. *J. Am. Chem. Soc.* **1964**, *86*, 5679−5680. (b) Saunders, M.; Schleyer, P. V. R.; Olah, G. A. Stable Carbonium Ions. XI.[1] The Rate of Hydride Shifts in the 2-Norbornyl Cation. *J. Am. Chem. Soc.* **1964**, *86*, 5680−5681. (c) Olah, G. A.; Prakash, G. K. S.; Arvanaghi, M.; Anet, F. A. L. High-Field ^{1}H and ^{13}C NMR Spectroscopic Study of the 2-Norbornyl Cation[1a]. *J. Am. Chem. Soc.* **1982**, *104*, 7105−7108. (d) Olah, G. A.; Prakash, G. K. S.; Saunders, M. Conclusion of the classical-nonclassical ion controversy based on the structural study of the 2-norbornyl cation. *Acc. Chem. Res.* **1983**, *16*, 440−448.

(8) (a) Yannoni, C. S.; Macho, V.; Myhre, P. C. Carbon-13 NMR Spectra of Carbonium Ions in the Solid State: The 2-Norbornyl Cation. *J. Am. Chem. Soc.* **1982**, *104*, 907−909. (b) Yannoni, C. S.; Macho, V.; Myhre, P. C. Resolved ^{13}C NMR Spectra of Carbonium Ions at Cryogenic Temperatures. The Norbornyl Cation at 5 K. *J. Am. Chem. Soc.* **1982**, *104*, 7380−7381.

(9) (a) Saunders, M.; Kates, M. R. Deuterium Isotope Effect on the Carbon-13 NMR Spectrum of the Bicyclo[2.2.1]heptyl Cation. Nonclassical Norbornyl Cation. *J. Am. Chem. Soc.* **1980**, *102*, 6867−6868. (b) Saunders, M.; Kates, M. R. Isotopic Perturbation Effects on a Single Averaged NMR Peak: Norbornyl Cation. *J. Am. Chem. Soc.* **1983**, *105*, 3571−3573. (c) Saunders, M.; Johnson, C. S., Jr. Effects of Tunneling on NMR Spectra. The Question of Heavy Atom Tunneling in Norbornyl Cations Reexamined. *J. Am. Chem. Soc.* **1987**, *109*, 4401−4402.

(10) Schleyer, P. V. R.; Sieber, S. The Classical 2-Norbornyl Cation Rigorously Defined *Ab Initio*. *Angew. Chem., Int. Ed.* **1993**, *32*, 1606−1608. and earlier references cited therein.

(11) Schreiner, P. R.; Severance, D. L.; Jorgensen, W. L.; Schleyer, P. V. R.; Schaefer, H. F. Energy Difference between the Classical and the Nonclassical 2-Norbornyl Cation in Solution. A Combined *ab Initio*-Monte Carlo Aqueous Solution Study. *J. Am. Chem. Soc.* **1995**, *117*, 2663−2664.

(12) Scholz, F.; Himmel, D.; Heinemann, F. W.; Schleyer, P. V. R.; Meyer, K.; Krossing, I. Crystal Structure Determination of the Nonclassical 2-Norbornyl Cation. *Science* **2013**, *341*, 62−64.

(13) Properzi, R.; Kaib, P. S. J.; Leutzsch, M.; Pupo, G.; Mitra, R.; De, C. K.; Song, L.; Schreiner, P. R.; List, B. Catalytic Enantiocontrol over a Non-Classical Carbocation. *Nat. Chem.* **2020**, *12*, 1174−1179.

(14) Frisch, M. J.; Trucks, G. W.; Schlegel, H. B.; Scuseria, G. E.; Robb, M. A.; Cheeseman, J. R.; Scalmani, G.; Barone, V.; Petersson, G. A.; Nakatsuji, H.; Li, X.; Caricato, M.; Marenich, A. V.; Bloino, J.; Janesko, B. G.; Gomperts, R.; Mennucci, B.; Hratchian, H. P.; Ortiz, J. V.; Izmaylov, A. F.; Sonnenberg, J. L.; Williams-Young, D.; Ding, F.; Lipparini, F.; Egidi, F.; Goings, J.; Peng, B.; Petrone, A.; Henderson, T.; Ranasinghe, D.; Zakrzewski, V. G.; Gao, J.; Rega, N.; Zheng, G.; Liang, W.; Hada, M.; Ehara, M.; Toyota, K.; Fukuda, R.; Hasegawa, J.; Ishida, M.; Nakajima, T.; Honda, Y.; Kitao, O.; Nakai, H.; Vreven, T.; Throssell, K.; Montgomery, J. A., Jr.; Peralta, J. E.; Ogliaro, F.; Bearpark, M. J.; Heyd, J. J.; Brothers, E. N.; Kudin, K. N.; Staroverov, V. N.; Keith, T. A.; Kobayashi, R.; Normand, J.; Raghavachari, K.; Rendell, A. P.; Burant, J. C.; Iyengar, S. S.; Tomasi, J.; Cossi, M.; Millam, J. M.; Klene, M.; Adamo, C.; Cammi, R.; Ochterski, J. W.; Martin, R. L.; Morokuma, K.; Farkas, O.; Foresman, J. B.; Fox, D. J. *Gaussian Revision*; Gaussian, Inc.: Wallingford, CT, 2016.

(15) Zhao, Y.; Truhlar, D. G. The M06 Suite of Density Functionals for Main Group Thermochemistry, Thermochemical Kinetics, Noncovalent Interactions, Excited States, and Transition Elements: Two New Functionals and Systematic Testing of Four M06-Class Functionals and 12 Other Functionals. *Theor. Chem. Acc.* **2008**, *120*, 215−241.

(16) Marenich, A. V.; Cramer, C. J.; Truhlar, D. G. Universal Solvation Model Based on Solute Electron Density and on a Continuum Model of the Solvent Defined by the Bulk Dielectric Constant and Atomic Surface Tensions. *J. Phys. Chem. B* **2009**, *113*, 6378−6396.

(17) Legault, C. Y. *CYLview, 1.0b*; Universite′ de Sherbrooke, 2009; http://www.cylview.org.

(18) (a) Singleton, D. A.; Hang, C.; Szymanski, M. J.; Greenwald, E. E. A New Form of Kinetic Isotope Effect. Dynamic Effects on Isotopic Selectivity and Regioselectivity. *J. Am. Chem. Soc.* **2003**, *125*, 1176−1177. (b) Ussing, B. R.; Hang, C.; Singleton, D. A. Dynamic Effects on the Periselectivity, Rate, Isotope Effects, and Mechanism of Cycloadditions of Ketenes with Cyclopentadiene. *J. Am. Chem. Soc.* **2006**, *128*, 7594−7607.

(19) Schreiner, P. R.; Schleyer, P. V. R.; Schaefer, H. F. III Why the Classical and Nonclassical Norbornyl Cations Do Not Resemble the 2-*endo*- and 2-*exo*-Norbornyl Solvolysis Transition States[1,†]. *J. Org. Chem.* **1997**, *62*, 4216−4228.

(20) Black, K.; Liu, P.; Xu, L.; Doubleday, C.; Houk, K. N. Dynamics, transition states, and timing of bond formation in Diels−Alder reactions. *Proc. Natl. Acad. Sci. U. S. A.* **2012**, *109*, 12860−12865.

https://doi.org/10.1021/acs.joc.3c02325
J. Org. Chem. 2024, 89, 1140−1146

(21) Pemberton, R. P.; Tantillo, D. J. Lifetimes of carbocations encountered along reaction coordinates for terpene formation. *Chem. Sci.* **2014**, *5*, 3301−3308.
(22) (a) Martínez, L.; Andrade, R.; Birgin, E. G.; Martínez, J. M. PACKMOL: A package for building initial configurations for molecular dynamics simulations. *J. Comput. Chem.* **2009**, *30*, 2157−2164. (b) Martínez, J. M.; Martínez, L. Packing optimization for automated generation of complex system's initial configurations for molecular dynamics and docking. *J. Comput. Chem.* **2003**, *24*, 819−825.

https://doi.org/10.1021/acs.joc.3c02325
J. Org. Chem. 2024, 89, 1140−1146